Molecular Structures of Some *syn*-[1.1]Metallocenophanes, *anti*-Ferrocenium[1.1]ruthenocenophane, and Their NMR Spectroscopies

Masanobu Watanabe,* Masaru Sato, Akira Nagasawa,† Izumi Motoyama,†† and Toshio Takayama††

Chemical Analysis Center, Saitama University, Urawa, Saitama 338

†Department of Chemistry, Faculty of Science, Saitama University, Urawa, Saitama 338

††Department of Applied Chemistry, Faculty of Engineering, Kanagawa University, Rokkakubashi, Yokohama 221

(Received March 13, 1998)

The structures of ferroceno[1.1]ruthenocenophane-1,13-dione (**1a**) and related compounds have been analyzed by X-ray diffraction. The crystal form of **1a** is orthorhombic, space group $Pbc2_1$, $a=6.0660(3)$, $b=13.371(1)$, $c=19.420(2)$ Å, $V=1575.1(2)$ Å^3, and the final $R=0.043$ and $R_w=0.054$. The air-oxidation of ferroceno[1.1]ruthenocenophane (**2a**) in xylene at 400 K gives ferroceno[1.1]ruthenocenophane-1-one (**3a**), implying the oxidation of the methylene group to a carbonyl group. The crystal form of **3a** is orthorhombic, space group $Pbn2_1$, $a=7.6460(7)$, $b=10.708(1)$, $c=19.587(2)$ Å, $V=1603.7(3)$ Å^3, and the final $R=0.052$ and $R_w=0.051$. The same oxidation is found for [1.1]ferrocenophane (**2b**) giving [1.1]ferrocenophane-1-one (**3b**). The crystal form of **3b** is orthorhombic, space group *Pbnm*, $a=7.5460(9)$, $b=10.6560(6)$, $c=19.8290(7)$ Å, $V=1594.4(2)$ Å^3, and the final $R=0.070$ and $R_w=0.077$. All the structural data of **1a**, **3a**, and **3b** showed their *syn* conformation about two bridging methylene groups and rigid structures caused by the good planarity of $C_5H_4COC_5H_4$ and $C_5H_4CH_2C_5H_4$ planes. These rigid structural features give remarkable variable temperature NMR (VT-NMR) spectra caused by the appropriate rate constant of $syn_a \Longleftrightarrow syn_b$ motion in solutions. The $\Delta G^{\ddagger}(T_c)$ values of the motion are estimated to be about 60 kJ mol^{-1}, which is more than six times larger than those of **2a** and **2b**. The *anti*-form of ferrocenium[1.1]ruthenocenophane formulated as $[Fe^{III}(C_5H_4CH_2C_5H_4)_2Ru^{II}]PF_6$ (**4**) was prepared by the oxidation of the *syn*-form **2a** in sulfuric acid containing NH_4PF_6. This is the first example of the oxidative occurrence of the conformational change from *syn*- to *anti*-form. The crystal form of **4** is triclinic, space group $P1$, $a=9.350(2)$, $b=10.777(3)$, $c=10.980(3)$ Å, $\alpha=91.84(3)°$, $\beta=96.66(2)°$, $\gamma=111.12(2)°$, $V=1021.8(5)$ Å^3 and the final $R=0.044$ and $R_w=0.048$. The cation contains largely twisted $C_5H_4CH_2C_5H_4$ plane (the twist angle, 34.1—38.5°) and largely tilted and rotated Cp-rings of the $Ru(C_5H_4)_2$ moiety.

The chemistry of ferroceno[1.1]ruthenocenophane (**2a**) and [1.1]ferrocenophane (**2b**), in which two metallocene moieties are linked together by two bridging methylene groups at the 1,1′-positions, has been studied from several points of view by Mueller–Westerhoff and his co-workers and other groups.[1—6] It has been known that the two conformations exist in [1.1]metallocenophanes from the molecule model, two methylene bridges can sit on the same side (*syn*-form) or on the opposite side (*anti*-form), but only the *syn*-conformation has been observed in the results of the X-ray diffraction studies for **2a**, **2b** and their related salts.[7—9] One of the structural features of **2a** and **2b** was found to be their twisted $C_5H_4CH_2C_5H_4$ ligands; i.e., the twisted angles, defined as the dihedral angle between the best plane of the two C_5H_4 rings of the $C_5H_4CH_2C_5H_4$ ligand, are 16.7 and 18.6° for **2a** and 12.7 and 13.8° for **2b**, which can relieve the steric hindrance between the inner α-hydrogens of the C_5H_4 rings.[7] No carbon bridged *anti*-[1.1]metallocenophane has even been prepared because of the large steric hindrance between the inner α-hydrogens. The distance between the two α-hydrogens would be about 0.8 Å if the $C_5H_4CH_2C_5H_4$ ligand could adopt a planar conformation.[10] However, two heteroatom bridged *anti*-[1.1]metallocenophanes were prepared, one is 1,1,12,12-tetrabutyl-1,13-distana[1.1]ferrocenophane[11] and the other is 1,1,12,12-tetramethyl-1,13-disila[1.1]ferrocenophane.[12] Much larger C_1–Sn (2.15 Å) and C_1–Si (1.861 Å) distances compared with C_1–CH_2 (about 1.50 Å) distance in *syn*-[1.1]-ferrocenophane (C_1 is defined as a bridged C atom) result in relief of the steric hindrance between the inner α-hydrogens.

In 1993, the first carbon bridged *anti*-[1.1]metallocenophane, *exo,exo*-1,13-dimethyl[1.1]ferrocenophane, was prepared.[13] Based on the results of the X-ray diffraction, two differences between the heteroatom-bridged *anti*-metallocenophanes and the carbon-bridged one are found; one is the large twisted structure of the $C_5H_4CH_2C_5H_4$ ligand and the other is the large tilted and rotated structure of the $Fe(C_5H_4)_2$ moiety. The twist angles are found to be 36.1° and 34.0° (0° for 1,1,12,12-tetramethyl-1,13-disila-[1.1]ferrocenophane) and the tilt and the rotation angles are 22.7° and 53.9°, respectively, for *anti*-1,13-dimethyl[1.1]-ferrocenophane. The large twisted, tilted, and rotated structure may relieve the steric hindrance of the inner α-hydrogens, which gives the formation of the carbon bridged *anti*-[1.1]metallocenophane.

On the other hand, the chemistry of ferroceno[1.1]-

ruthenocenophane-1,13-dione (**1a**) and related compounds (**1b**, **3a**, **3b**) has been rare because of their poor yield (yield of **2b**, 3.5%[6]), their poor solubility (**1a**, **1b**) in the organic solvent, and their higher oxidation potential (both diones were not oxidized by iodine and H_2SO_4 in air, in this study). Although no VT-NMR spectra are observed for **2a** and **2b** due to the extremely fast $syn_a \Longleftrightarrow syn_b$ exchange motion in solution,[1] the compounds **1a**, **1b**, **3a**, and **3b** gave VT-NMR spectra due to the structures less flexible than those of **2a** and **2b**. One of the aims of this study is to investigate the crystal structures of **1a**, **3a**, and **3b** in order to explain the VT-NMR spectra from the viewpoint of structural chemistry. The other is to show the crystal structure of the first *anti*-formed paramagnetic ferrocenium salt **4**, which is obtained from the oxidation of **2a** in sulfuric acid, comparable with those of the reported *anti*-form of [1.1]metallocenophanes (Scheme 1).

Experimental

Syntheses. Compounds **1a**, **1b**, **2a**, and **2b** were prepared by the methods reported previously.[4,14] Compounds **3a** and **3b** were prepared as follows; **2a** (100 mg, 0.23 mmol) was dissolved in xylene (50 cm^3) at room temperature under air. The solution was heated at 130 °C for 2 h, the yellow color of the solution changed into orange-red, gradually. The solution was filtered and evaporated. The crude product was separated by column chromatography on alumina. The starting compound was eluted by a mixture of hexane and benzene (1 : 1) as a yellow band, which was recrystallized from hexane as yellow precipitates (about 75 mg). Compound **3a** was eluted by a mixture of benzene–ether (3 : 1) as an orange-yellow band and was recrystallized from mixed solution of benzene and hexane to give orange-red crystals (12 mg, 0.026 mmol, yield 11.6%). Found: C, 58.11; H, 3.92%. Calcd for $C_{22}H_{18}FeORu$: C, 58.04; H, 3.99%. Compound **3b** was prepared by a method similar to that used for **3a** (yield 12%). Found: C, 64.31; H, 4.32%. Calcd for $C_{22}H_{18}Fe_2O$: C, 64.44; H, 4.42%. Salt **4** was prepared as follows: **2a** (100 mg, 0.23 mmol) was added to concentrated sulfuric acid (20 cm^3) at room temperature. The yellow color of the solution changed into blue-green immediately, and gas was evolved. After the solution has been left to stand for 30 min, it was poured into ice water. After filtration of the solution, a concentrated aqueous solution of NH_4PF_6 was added, and black precipitates **4** were formed. The precipitates were recrystallized from the CH_3CN–$C_2H_5OC_2H_5$ mixture (79 mg, 0.14 mmol, yield 59.5%). Found: C, 45.31; H, 3.22%. Calcd for $C_{22}H_{20}F_6FePRu$: C, 45.07; H, 3.44%. Salt **8** was prepared using compound **2b** by a method similar to that used for **4**. Found: C, 48.78; H, 3.45%. Calcd for $C_{22}H_{19}F_6Fe_2P$: C, 48.93; H, 3.55%.

NMR Measurement and X-Ray Analysis. The ^1H NMR spectra (400.134 MHz) were recorded at 298 K on a Bruker AM400 instrument and referred to TMS as the internal standard. ^{57}Fe-Mössbauer spectroscopies were done under the same conditions as for the previously report.[9]

Single crystals suitable for X-ray studies were obtained by recrystallization from toluene (**1a**) and from a mixture of benzene and hexane (**3a**, **3b**). The single crystals of **4** were obtained by diffusion of ether vapor into CH_3CN solution at about 260 K. X-Ray intensities were recorded on a MAX Science DIP3000 image processor with graphite-monochromated Mo $K\alpha$ radiation and a 18-kW rotating-anode generator. All the structures were solved with the Dirdif–Patty method in CRYSTAN-GM (software-pack for

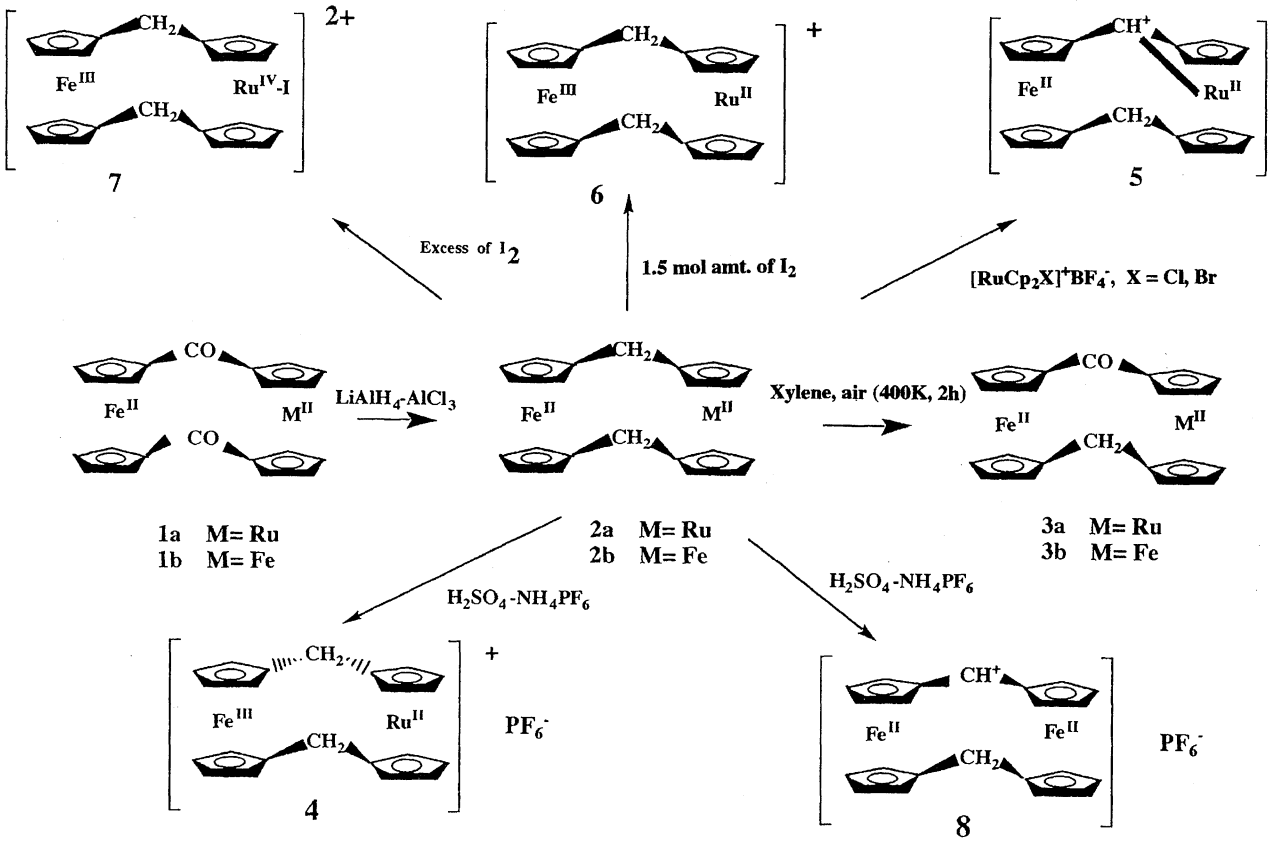

Scheme 1.

structure determination) and refined finally by the full-matrix least squares procedure. An anisotropic refinement for non-hydrogen atoms was done and all the hydrogen atoms, partially located from difference Fourier maps, were isotropically refined.

Attempts to solve the structure of **4** using space group $P\bar{1}$ or $P1$ have been carried out, however, the attempt using centrosymmetric structure $P\bar{1}$ has not been refined well. The crystallographic data for **1a**, **3a**, **3a**, and **4** and the experimental conditions for the X-ray structure analysis are listed in Table 1. Tables of the atomic coordinates thermal parameters, bond distances, and $F_o - F_c$ data for **1a**, **3a**, **3a**, and **4** are deposited as Document No. 71044 at the Office of the Editor of Bull. Chem. Soc. Jpn.

Results and Discussion

The Structures of 1a, 3a, and 3b. Compound **1a** crystallized in the orthorhombic space group $Pbc2_1$. The selected interatomic distances for **1a** are shown in Table 2. The ORTEP drawing of **1a** is showed in Fig. 1, with the atom-numbering scheme.

The X-ray diffraction study showed that the conformation of **1a** was the *syn*-form, similarly to **2a**, **2b** and their related salts;[7–9] no change of the *syn*-conformation occurred during the reduction of dione **1a** to alkane **2a** with $LiAlH_4/AlCl_3$.

Two structural features were found for **1a**: One is the averaging of the M–Cp distances. The mean Fe(1)–C_{ring} and Fe(1)–Cp distances were 2.10(4) and 1.702(8) Å, respectively, which were longer by about 0.06 Å than the corresponding values of ferrocene (2.045, 1.65 Å[15]) and **2a** (2.043(4), 1.647(6) Å[7]), respectively. The mean Ru(1)–C_{ring} and Ru(1)–Cp distances were 2.13(3) and 1.762(8) Å, respectively, which were shorter by about 0.07 Å than the values for ruthenocene (2.21, 1.84 Å[16]) and [1.1]ruthenocenophane (2.187(7), 1.819(4) Å[7]), respectively. These averaged

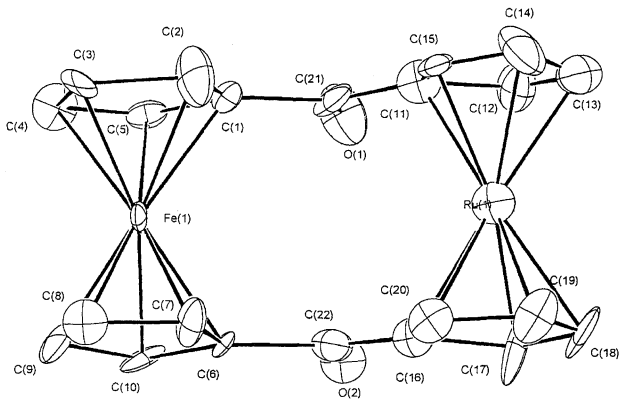

Fig. 1. ORTEP drawing of **1a** with the numbering scheme of the atoms.

M–Cp distance should be caused by the two conjugated $C_5H_4COC_5H_4$ planes, because both planes keep a good planarity (twist angles, 0.9° for the planes C(1)–C(5) and C(11)–C(15), 1.0° for the planes C(6)–C(10) and C(16)–C(20)). The two Cp-rings of $Fe(C_5H_4)_2$ and $Ru(C_5H_4)_2$ moieties were almost parallel to each other (tilt angle: 2.5° for the $Fe(C_5H_4)_2$ moiety, 3.6° for the $Ru(C_5H_4)_2$ moiety). These features give the good eclipsed structures of $M(C_5H_4)_2$ moieties. These structural features are in contrast to those of **2a**[7] the two $C_5H_4CH_2C_5H_4$ ligands of which are twisted strongly (average twist angle; 17.7°) with each other in order to reduce the steric hindrance between the inner α-hydrogens, as described in the Introduction.

The other structural feature was found in the bridge angles of C_1–CO–C_1 (122(1)° for C(1)–C(21)–C(11) and 123(2)° for C(6)–C(22)–C(16)), which were somewhat larger than

Table 1. Crystal and Intensity Collection Data

	1a	**3a**	**3b**	**4**
Formula	$C_{22}H_{16}FeO_2Ru$	$C_{22}H_{18}FeORu$	$C_{22}H_{18}Fe_2O$	$C_{22}H_{20}Fe_6FePRu$
Formula weight	469.28	455.30	410.07	586.28
Cryst. size/mm	$0.22\times0.15\times0.08$	$0.12\times0.12\times0.05$	$0.35\times0.21\times0.15$	$0.21\times0.32\times0.32$
Crystal system	Orthorhombic	Orthorhombic	Orthorhombic	Triclinic
Space group	$Pbc2_1$	$Pbn2_1$	$Pbnm$	$P1$
a/Å	6.0660(3)	7.6460(7)	7.5460(9)	9.350(2)
b/Å	13.371(1)	10.708(1)	10.6560(6)	10.777(3)
c/Å	19.420(2)	19.587(2)	19.8290(7)	10.980(3)
α/°	—	—	—	91.84(3)
β/°	—	—	—	96.66(2)
γ/°	—	—	—	111.12(2)
V/Å^3	1575.1(2)	1603.7(3)	1594.4(2)	1021.8(5)
Z	4	4	4	2
D_x/g cm^{-3}	1.984	1.885	1.708	1.905
μ/cm^{-1}	18.81	18.35	18.26	15.72
Radiation	Mo $K\alpha$	Mo $K\alpha$	Mo $K\alpha$	Mo $K\alpha$
No. of ref.	2593	2747	2525	5086
No. of obs.	1937 ($I>2.0\ \sigma(I)$)	1044 ($I>3.0\ \sigma(I)$)	1170 ($I>2.0\ \sigma(I)$)	4180 ($I>2.0\ \sigma(I)$)
Index range	$0<h<7$	$0<h<10$	$0<h<10$	$-12<h<12$
	$0<k<18$	$0<k<25$	$0<k<14$	$-13<k<13$
	$0<l<27$	$0<l<27$	$0<l<28$	$0<l<14$
R	0.043	0.052	0.070	0.044
R_w	0.054	0.051	0.077	0.048

Table 2. Selected Bond Distances for **1a**, **3a**, and **3b**

Atom 1 Atom 2	Dist./Å	Atom 1 Atom 2	Dist./Å
For **1a**			
Fe(1)–C(1)	2.18(3)	Ru(1)–C(11)	2.08(3)
Fe(1)–C(2)	2.16(3)	Ru(1)–C(12)	2.13(2)
Fe(1)–C(3)	2.07(3)	Ru(1)–C(13)	2.11(3)
Fe(1)–C(4)	2.08(3)	Ru(1)–C(14)	2.17(3)
Fe(1)–C(5)	2.11(2)	Ru(1)–C(15)	2.08(3)
Fe(1)–C(6)	2.09(2)	Ru(1)–C(16)	2.14(3)
Fe(1)–C(7)	2.08(2)	Ru(1)–C(17)	2.17(2)
Fe(1)–C(8)	2.14(3)	Ru(1)–C(18)	2.17(3)
Fe(1)–C(9)	2.05(3)	Ru(1)–C(19)	2.11(3)
Fe(1)–C(10)	2.05(2)	Ru(1)–C(20)	2.14(3)
O(1)–C(21)	1.25(1)	O(2)–C(22)	1.24(1)
C(1)–C(21)	1.25(1)	C(6)–C(22)	1.57(3)
C(11)–C(21)	1.52(4)	C(16)–C(22)	1.37(4)
For **3a**			
Fe(1)–C(1)	2.06(4)	Ru(1)–C(11)	2.13(3)
Fe(1)–C(2)	1.94(4)	Ru(1)–C(12)	2.12(2)
Fe(1)–C(3)	2.02(4)	Ru(1)–C(13)	2.10(3)
Fe(1)–C(4)	2.21(4)	Ru(1)–C(14)	2.14(3)
Fe(1)–C(5)	2.12(3)	Ru(1)–C(15)	2.16(3)
Fe(1)–C(6)	2.10(4)	Ru(1)–C(16)	2.16(3)
Fe(1)–C(7)	2.20(4)	Ru(1)–C(17)	2.12(2)
Fe(1)–C(8)	2.15(4)	Ru(1)–C(18)	2.11(3)
Fe(1)–C(9)	2.02(5)	Ru(1)–C(19)	2.04(3)
Fe(1)–C(10)	2.06(5)	Ru(1)–C(20)	2.00(3)
O(1)–C(21)	1.23(3)	C(1)–C(21)	1.55(5)
C(6)–C(22)	1.50(6)	C(11)–C(21)	1.40(6)
C(16)–C(22)	1.49(5)		
For **3b**			
Fe(1)–C(1)	2.08(1)	Fe(1)–C(2)	2.08(1)
Fe(1)–C(3)	2.04(1)	Fe(1)–C(4)	2.03(1)
Fe(1)–C(5)	2.06(1)	Fe(1)–C(6)	2.05(1)
Fe(1)–C(7)	2.06(1)	Fe(1)–C(8)	2.06(1)
Fe(1)–C(9)	2.05(1)	Fe(1)–C(10)	2.04(1)
O(1)–C(12)	1.22(1)	C(1)–C(11)	1.50(1)
C(6)–C(12)	1.47(1)		

the sp^2-hybridized C atom (120°), resulting in relief of the steric hindrance between the inner α-hydrogens; i.e., the distances between the H(2)···H(15) and H(7)···H(20) were 1.99 and 2.06 Å, respectively, (although they are smaller than the sum (2.4 Å) of the van der Waals radii of H atom[18]). The large bridge angle gives a longer Fe···Ru distance (4.836(3) Å) than **2a** (4.792(2) Å). The distances C(21)–O(1) and C(22)–O(2) were found to be 1.25(1) and 1.24(1) Å, respectively, which are close to the reported CO bond distance of α-keto-1,1′-trimethylene[3]ferrocenophane (1.211 Å).[19]

The reduction of **1a** with $AlCl_3$–$LiAlH_4$ gives **2a**. As mentioned in the Experimental section, yellow color of **2a** in xylene changes into red-orange during heating under air. The separation of the crude products by chromatography gave **3a** as orange-red precipitates. The IR spectrum of **3a** showed the presence of CO group (ν_{CO}, 1606 cm^{-1}). The same reaction was observed for **2b** to give **3b** (ν_{CO}, 1598 cm^{-1}). The latter compound was already prepared by oxidation of **2b** with active MnO_2 in a higher yield (86%).[5] These facts are comparable with the reported fact that the reaction of **2a** with haloruthenocenium cation $[RuCp_2X]^+$ (X = Br, Cl) gave the α-carbocation **2a**$^+$ (**5**) with the stable Ru–C$^+$ bond,[9] indicating that the methylene group of **2a** was easily oxidized giving the α-carbocation. In this study, the methylene group was also oxidized under air, giving a carbonyl group at higher temperature; i.e., the driving force of both reactions may be ascribed to the facility of the formation of the metallocenyl carbocation $CpMC_5H_4C^+$.

Both compounds **3a** and **3b** were crystallized, in the orthorhombic space group $Pbc2_1$ and *Pbnm*, respectively. The selected interatomic distances for **3a** and **3b** are given in Table 2 and the ORTEP drawings of **3a** and **3b** are shown in Figs. 2 and 3, respectively, with the atom numbering system.

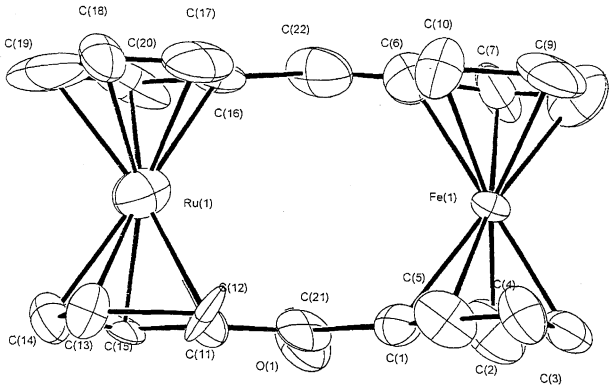

Fig. 2. ORTEP drawing of **3a** with the numbering scheme of the atoms.

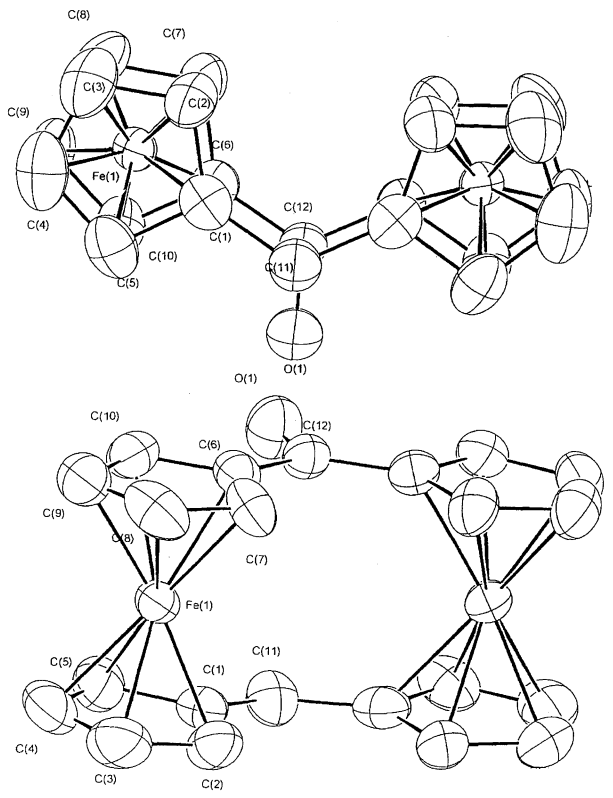

Fig. 3. ORTEP drawing of **3b** with the numbering scheme of the atoms.

The conformation of **3a** was also a syn-form. All the structural data of **3a** were more closer to those of **1a** than **2a**. The averaged M–Cp distance and the large bridge angles were also found in spite of the involvement of a flexible $C_5H_4CH_2C_5H_4$ group in **3a**. The mean Fe(1)–C_{ring} and Fe(1)–Cp distances were 2.09(7) and 1.700(9) Å, respectively, and the mean Ru(1)–C_{ring} and Ru(1)–Cp distances were 2.11(5) and 1.728(9) Å, respectively, close to the corresponding values of **1a** (see Table 3).

These structural features were likely caused by the good planarity of $C_5H_4COC_5H_4$ (twist angle, 0.9°) and $C_5H_4CH_2C_5H_4$ (5.2°). The latter value is much smaller than the 17.7° of **2a**. The two C_5H_4-ring of $Fe(C_5H_4)_2$ and $Ru(C_5H_4)_2$ moieties were almost parallel (tilt angle, 1.7° and 4.8° for the $Fe(C_5H_4)_2$ and $Ru(C_5H_4)_2$ moieties, respectively), and the two C_5H_4-rings of both moieties were eclipsed. The inner α-hydrogens distances (1.93 for H(5)···H(12) and 2.00 Å for H(10)···H(17)) were shorter than the sum of van der Waals radii of H atoms, giving large bridge angles of C_1–CO–C_1 (124(2)°) and C_1–CH_2–C_1 (122(2)°). The Fe and Ru distance (4.797(4) Å) is somewhat shorter than the value of **1a** (4.836(3) Å). The distance of C(21)–O(1) was found to be 1.23(3) Å.

Figure 3 shows the ORTEP drawing of **3b**. The C(11), C(12), and O(1) atoms were located on the crystallographic mirror plane at x, 1/4, z; the molecule of **3b** had a C_{2v} symmetry. The conformation of **3b** was also *syn*-form. The mean Fe(1)–C_{ring} and Fe(1)–Cp distances were 2.05(2) and 1.660(5) Å, respectively, which were close to the corresponding values of ferrocene and smaller than those of **1a** and **3a**. The Fe···Fe distance (4.807(1) Å) is also close to the value of **3a**. The planes of $C_5H_4COC_5H_4$ and $C_5H_4CH_2C_5H_4$ were almost planar. The two C_5H_4-rings of the $Fe(C_5H_4)_2$ moieties in **3b** were almost parallel to each other (tilt angle, 3.4°), and the two C_5H_4-rings were eclipsed. The bridge angles of C(1)–C(11)–C(1)* (122(1)°) and C(6)–C(22)–C(6)* (123(1)°) were comparable with those in **1a** and **3a**. The distance of C(21)–O(1) was found to be 1.22(1) Å.

The interesting structural feature found in **3a** and **3b** compared with those of dione (**1a**) and alkanes (**2a** and **2b**) was the presence of some interaction, probably a hydrogen bond (it has been pointed that the distance below about 3 Å suggests a hydrogen bond[20]) between the CO group in $C_5H_4COC_5H_4$ and the CH_2 group in $C_5H_4CH_2C_5H_4$; i.e., the shortest O···H distances between the CH_2 and CO groups of **3a** and **3b** were found to be 2.93 and 2.71 Å, respectively, the latter was within the range of the O···H hydrogen bond distance (2.76 (ice), 2.74 ($B(OH)_3$), 2.67 Å ($HCOOH)_2$).[20]

All the results of the X-ray diffraction studies of **1a**, **3a**, and **3b** showed that they existed in a *syn*-conformation. Compared with the structure of analogs **2a** and **2b**, their structural features were found in their rigid structure caused by the good planarity of the $C_5H_4COC_5H_4$ and $C_5H_4CH_2C_5H_4$ planes and some interaction between the bridging CO and CH_2 groups. These rigid structures of compounds **1a**, **3a**, and **3b** give an appropriate higher activation energy of the $syn_a \Longleftrightarrow syn_b$ exchange in solution and unusual VT-NMR spectra described below in detail.

NMR Studies of 1a, 1b, 3a, and 3b. Figure 4a shows the VT ^{1}H NMR spectra of **1a** in $CDCl_3$ and the δ values and their assignment are listed in Table 4. Three sharp and one broad signals were observed at 330 K. The two sharp signals at $\delta = 5.55$ and 4.76 were assigned to the α- and β-ring protons of the $Ru(C_5H_4)_2$ moiety, respectively, and other signals at $\delta = 4.94$ and 4.58 assigned to the α- and β-ring protons of the $Fe(C_5H_4)_2$ moiety, respectively. Like **2a** and **2b**, α- and β-protons of the metallocenes appeared as singlets due to the fast $syn_a \Longleftrightarrow syn_b$ motions at high temperature. Upon cooling, these signals broadened, and eight new sharp signals appeared and the signals became distinguishable at 220 K. The four-signals ascribed to the $Ru(C_5H_4)_2$ moiety and four signals to the $Fe(C_5H_4)_2$ moiety were observed (the δ values are shown in Table 4). This phenomenon is in a sharp contrast to that in **2a** under the same conditions. For **2a**, two sharp signals (4.68 (α-protons), 4.54 (β-protons)) for the Ru-$(C_5H_4)_2$ moiety and two signals (4.21 (α-protons), 4.08 (β-protons)) for the $Fe(C_5H_4)_2$ moiety were observed for all the temperatures because of the fast $syn_a \Longleftrightarrow syn_b$ exchange motion. Mueller-Westerhoff estimated the barrier of the motion to be less than 10 kJ mol^{-1} for **2a** and **2b**.[1] The rigid struc-

Table 3. Selected Bond Distances and Angles of **1a**, **3a**, **3b**, and **4**

	1a	**3a**	**3b**	**4**	
				Cation **A**	Cation **B**
Fe–Cp	1.702(8)	1.700(9)	1.660(5)	1.703(8)	1.698(9)
Ru–Cp	1.762(8)	1.728(9)	—	1.809(3)	1.828(9)
Fe–C_{ring}	2.10(4)	2.09(7)	2.05(2)	2.07(3)	2.08(6)
Ru–C_{ring}	2.13(3)	2.11(5)	—	2.17(4)	2.19(5)
M···M	4.836(3)	4.797(4)	4.807(1)	4.608(2)	4.597(2)
Bride angle C_1–CH_2–C_1		122(2)	122(1)	118(1), 121(1)	120(1), 122(1)
C_1–CO–C_1	122(1), 123(2)	124(2)	123(1)	—	—
Twist angle $C_5H_4CH_2C_5H_4$		5.2	0	34.1, 38.2	35.1, 38.5
$C_5H_4COC_5H_4$	0.9, 1.0	0.9	0	—	—
Tilt angle $Fe(C_5H_4)_2$ moiety	2.5	1.7	3.4	2.6	4.0
$Ru(C_5H_4)_2$ moiety	3.6	4.8	—	12.7	8.5

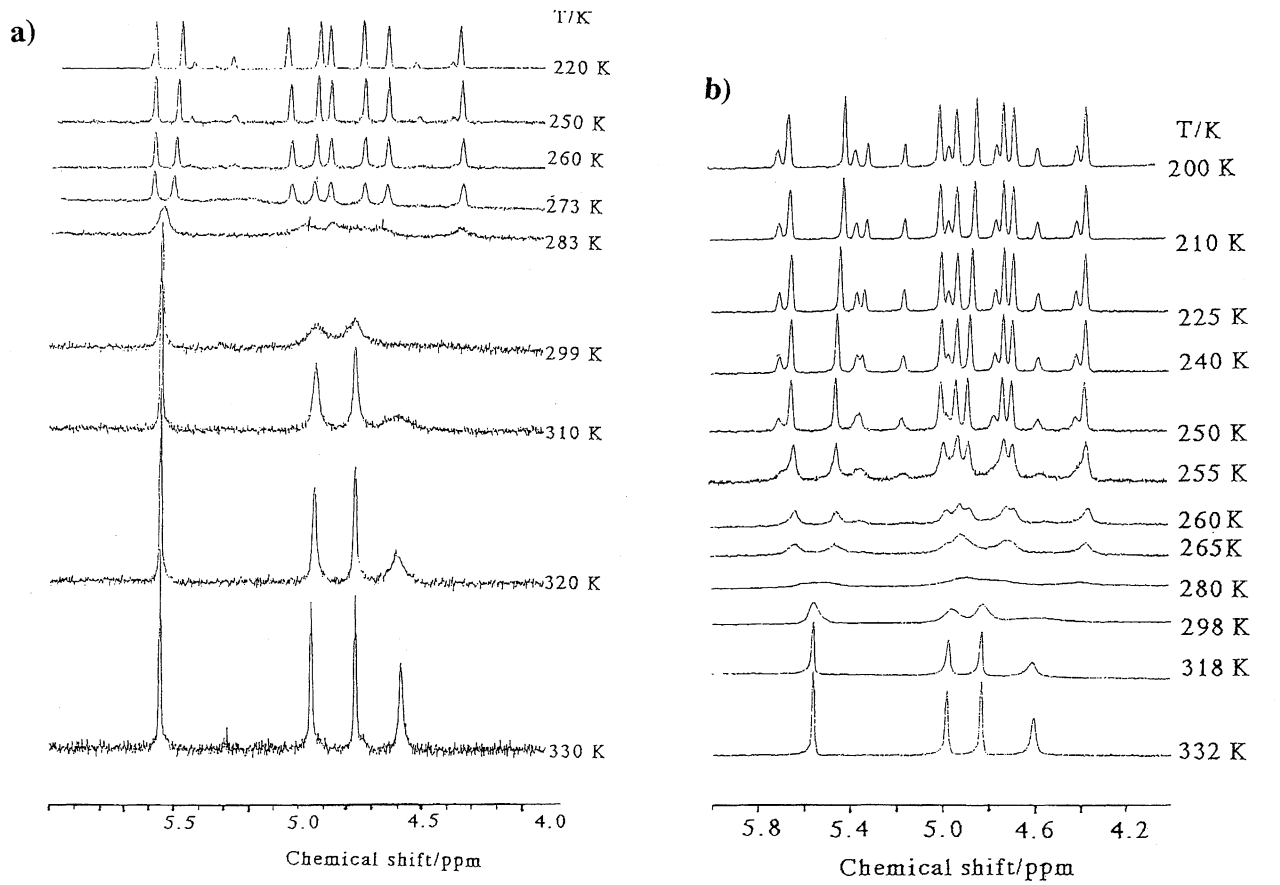

Fig. 4. ^{1}H NMR spectra of **1a** in $CDCl_3$ (**a**) and $CDCl_3/CD_3COCD_3$ (**b**) at indicated temperatures.

ture of **1a** caused by the two planar $C_5H_4COC_5H_4$ groups was the higher barrier to the motion. The activation parameters for the motion of **1a**, **1b**, **3a**, and **3b** are estimated from the change of the α-proton signals of the $Fe(C_5H_4)_2$ moiety because they afforded well-separated signals for all the compounds. The T_c is about 283 K for **1a**. The lifetime (τ/s) of the motion is estimated to be 6.6×10^{-3} s at T_c from the equation $\tau = 2^{1/2}\delta^{-1}\pi^{-1}$, where δ(Hz) is the difference in the chemical shift between the signals at the 2- and 5-positions (0.17 ppm; 68 Hz). The value of the activation energy at T_c ($\Delta G^{\ddagger}(T_c)$) was estimated to be 57(2) kJ mol^{-1} from the equation $\Delta G^{\ddagger}(T_c) = 2.303\ RT_c\ (10.319 + \log\tau + \log T_c)$.

The same VT-NMR spectra have been observed for **1b**, and the T_c for the α-protons (about 285 K) was somewhat higher than that of **1a**. The values of τ and $\Delta G^{\ddagger}(T_c)$ were estimated to be 18.7×10^{-3} s and 60(2) kJ mol^{-1}, respectively. The $\Delta G^{\ddagger}(T_c)$ values of **1a** and **1b** were much larger than the values of the alkanes (**2a** and **2b**), that gave the VT-NMR spectra.

The most striking spectral feature of **1a** was the appearance of four new and small signals (δ = 5.46, 5.26, 4.53, 4.38, an intensity ratio about 13%) at lower temperatures (< 250 K, see Fig. 4a) and this spectral feature was reproducible. The same spectral feature had been also reported for **1b**. At first, we assigned the signals to the *anti*-form of **1b**,[21] however considering the results of present and reported studies, they may be ascribed to the twist-form (see Scheme 2) defined as an intermediate state between syn_a to syn_b reported for Muller-Westerhoff[1] for the following reasons. One is that no evidence have been reported of the conformational change from the *syn* to *anti* form of [1.1]metallocenophane in solution at lower temperatures. Two is the fact that the single crystals of **1a** and **1b** (perfect *syn*-form) gave the same ^{1}H VT-NMR spectra in solution; i.e., the small signals are not due to the *anti*-form. Third is the fact that the new signals are observed for only the tight structures of dione (**1a** and **1b**) at lower temperatures. The tight structure of **1a** and **1b** may give the appropriate lifetime of the twist conformer for an NMR time scale at lower temperature, thus their NMR signals are observed at lower than 250 K.

From the molecule model of the twist form of **1a** and **1b**, the eight and four signals should be observed, respectively. Actually **1b** gave four signals at 220 K in $CDCl_3$, however the eight signals were not observed independently in $CDCl_3$ for **1a** because of the superimposed of some signals of the twist conformer to the main signal. Thus, the eight signals for **1a** should be observed in solutions other than $CDCl_3$. Figure 4b shows the VT-NMR spectra of **1a** in the mixed solution of $CDCl_3$–CD_3COCD_3 (1/1). The values of T_c, τ, and $\Delta G^{\ddagger}(T_c)$, were estimated to be about 270 K, 14.1×10^{-3} s and 56(2) kJ mol^{-1}. At lower temperatures, new and small intensities eight signals assigned to the twist conformer (δ values and their assignment are shown in Table 4) were observed.

A similar VT-NMR spectrum was expected for **3a** in

Table 4. ^{1}H-Chemical Shifts of **1a**, **1b**, **3a**, and **3b**

Compounds	Temp/K	1H Chemical shift/ppm	Assignment	
1a[a]	330	5.55, 4.76	α-, β-protons	$Ru(C_5H_4)_2$
		4.94, 4.58	α-, β-protons	$Fe(C_5H_4)_2$
	220	5.57, 5.46	α-protons	$Ru(C_5H_4)_2$
		4.91, 4.72	β-protons	$Ru(C_5H_4)_2$
		5.04, 4.87	α-protons	$Fe(C_5H_4)_2$
		4.63, 4.35	β-protons	$Fe(C_5H_4)_2$
		5.46, 5.26, 4.53, 4.38	Twist structure	
1a[b]	330	5.55, 4.83	α-, β-protons	$Ru(C_5H_4)_2$
		4.98, 4.60	α-, β-protons	$Fe(C_5H_4)_2$
	200	5.65, 5.40	α-protons	$Ru(C_5H_4)_2$
		4.83, 4.72	β-protons	$Ru(C_5H_4)_2$
		5.00, 4.92	α-protons	$Fe(C_5H_4)_2$
		4.67, 4.36	β-protons	$Fe(C_5H_4)_2$
		5.70, 5.36, 4.96, 4.75	Twist structure	$Ru(C_5H_4)_2$
		5.30, 5.14, 4.58, 4.40	Twist structure	$Fe(C_5H_4)_2$
1b[a]	330	5.25, 4.49	α-, β-protons	$Fe(C_5H_4)$
	220	5.36, 5.30	α-protons	$Fe(C_5H_4)_2$
		4.61, 4.44	β-protons	$Fe(C_5H_4)_2$
		5.23, 5.18, 4.93, 4.36	Twist structure	$Fe(C_5H_4)_2$
3a[a]	330	5.31, 4.82	α, β-protons	$Ru(C_5H_4CO)$
		4.97, 4.48	α, β-protons	$Fe(C_5H_4CO)$
		4.79, 4.56	α, β-protons	$Ru(C_5H_4CH_2)$
		4.23, 4.11	α, β-protons	$Fe(C_5H_4CH_2)$
		3.05		$-CH_2-$
	210	5.32, 5.25	α-protons	$Ru(C_5H_4CO)$
		4.89, 4.87	β-protons	$Ru(C_5H_4CO)$
		4.97, 4.94	α-protons	$Fe(C_5H_4CO)$
		4.55, 4.53	β-protons	$Fe(C_5H_4CO)$
		4.82, 4.73	α-protons	$Ru(C_5H_4CH_2)$
		4.60, 4.55	β-protons	$Ru(C_5H_4CH_2)$
		4.30, 4.24	α-protons	$Fe(C_5H_4CH_2)$
		4.22, 4.06	β-protons	$Fe(C_5H_4CH_2)$
		3.19, 2.77		$-CH_2-$
3b[a]	330	4.99, 4.39	α-, β-protons	$Fe(C_5H_4CO)$
		4.53, 4.13	α-, β-protons	$Fe(C_5H_4CH_2)$
		3.04		$-CH_2-$
	210	5.00, 4.95	α-protons	$Fe(C_5H_4CO)$
		4.49, 4.30	β-protons	$Fe(C_5H_4CO)$
		4.58, 4.55	α-protons	$Fe(C_5H_4CH_2)$
		4.18, 4.10	β-protons	$Fe(C_5H_4CH_2)$
		3.07, 2.90		$-CH_2-$

a) in $CDCl_3$. b) in mixed solutions of $CDCl_3$ and CD_3COCD_3 (1/1).

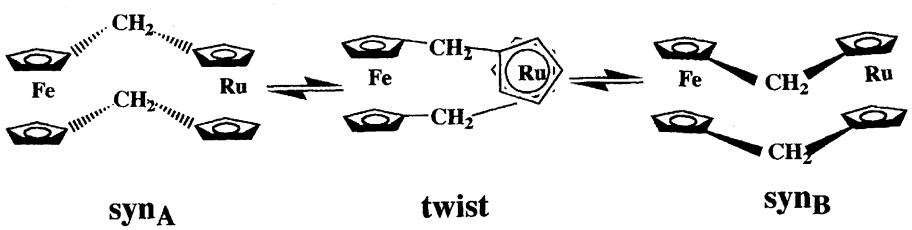

Scheme 2.

$CDCl_3$ because of its rigid structure. In **3a**, nine sharp signals were observed at 330 K. Upon cooling, the nine signals were broadened, new sharp eighteen signals were observed at 255 K, and the signals became distinguishable at 210 K. The T_c value of the α-protons of $C_5H_4COC_5H_4$-ring of the $Fe(C_5H_4)_2$ side is about 260 K and the values of τ and

$\Delta G^{\ddagger}(T_c)$, are estimated to be 37×10^{-3} s and 56(2) kJ mol^{-1}. The interesting point is found in the $\delta = 3.05$ ascribed to the methylene group; i.e., the signal shifts to higher field by about 0.5 ppm compared with that of **2a**. The shift must be caused by the shielding effect of the CO group because the methylene group sits above the CO group as shown by the result of X-ray diffraction. At 210 K, the methylene signals were observed at $\delta = 3.19$ (d, outer proton, $J_{H-H} = 20$ Hz) and 2.77 (d, inner proton, $J_{H-H} = 20$ Hz). This coupling constant is somewhat larger than the value of normal geminal CH_2 (12—15 Hz) and close to the corresponding value in α-carbocation **2a**$^+$ ($J_{H-H} = 22$ Hz[9]) and **2b**$^+$ ($J_{H-H} = 22$ Hz[1]), indicating an sp^2 character.

The similar VT-NMR spectrum was reported for **3b**.[21] The T_c value of α-protons of $C_5H_4COC_5H_4$-ring of $Fe(C_5H_4)_2$ moiety was about 297 K and this is 37 K larger than the value of **3a**. The values of τ and $\Delta G^{\ddagger}(T_c)$ were estimated to be 23×10^{-3} and 63(2) kJ mol^{-1}.

The most interesting spectral features found in **3a** and **3b** compared with **1a** and **1b** were the absence of the new signals ascribed to the twist conformation at lower temperatures. The absence of the spectra may be deeply involved with the presence of the hydrogen bond interaction between the CO and CH_2 groups in **3a** and **3b**, which may reduce the lifetime of the twist conformer greatly because such a hydrogen bond is considered to be absent in the twist conformer.

All the results obtained here indicate clearly that the less flexible structures of **1a**, **1b**, **3a**, and **3b** than **2a** and **2b** gave the VT-NMR spectra caused by the appropriate rate constant of $syn_a \Longleftrightarrow syn_b$ motions.[1] The $\Delta G^{\ddagger}(T_c)$ values of the motion for **1a**, **1b**, **3a**, and **3b** are estimated to be about 60 kJ mol^{-1}, which is more than six times larger than the values for **2a** and **2b**.

The Structure of 4. The salt **4** crystallized in the triclinic space group $P\bar{1}$ and the selected interatomic distances for **4** are shown in Table 5. The ORTEP drawing of the cation is illustrated in Fig. 5, with the atom numbering system.

The unit cell had two independent cations (unit **A**, Ru(1)Fe(1) and unit **B**, Ru(2)Fe(2)). The structure of cation **A**, having a similar structure of **B**, is discussed in detail. The mean Fe(1)–C_{ring} and Fe(1)–Cp distances were 2.07(3) and 1.703(8) Å, respectively, which were longer than the corresponding values of ferrocene[14] and **2b**[7] and close to the values of ferrocenium cation (2.075, 1.70 Å[22]), indicating the formal oxidation state of Fe^{III}. The mean Ru(1)–C_{ring} and Ru(1)–Cp distances were 2.17(4) and 1.809(3) Å, respectively, which correspond well with the values of ruthenocene (2.21 and 1.84 Å) and [1.1]-ruthenocenophane (2.187(7) and 1.819(4) Å[7]), respectively, implying the formal oxidation state of Ru^{II}. As the result, the formula $[Fe^{III}(C_5H_4CH_2C_5H_4)_2Ru^{II}]^+PF_6^-$ is given for **4**. The formulation is comparable with the result of the ^{57}Fe–Mössbauer spectroscopy in which typical broad ferrocenium-like Mössbauer single peaks were observed at all the temperatures (78—300 K) (isomer shift 0.49 and 0.43 mm s^{-1} at 78 and 300 K, respectively).

The most striking structural feature of the cation of **4** is the *anti*-conformation unlike the original metallocenophane **2a** and related compounds (**1a**, **1b** and the previously reported α-carbonium [1.1]metallocenophanes). To our knowledge, **4** is the first salt identified as the *anti*-[1.1]-

Table 5. Selected Bond Distances for **4**

Atom 1 Atom 2	Dist./Å	Atom 1 Atom 2	Dist./Å
Fe(1)–C(1)	2.06(1)	Ru(1)–C(11)	2.24(1)
Fe(1)–C(2)	2.08(1)	Ru(1)–C(12)	2.16(1)
Fe(1)–C(3)	2.07(1)	Ru(1)–C(13)	2.20(1)
Fe(1)–C(4)	2.01(1)	Ru(1)–C(14)	2.12(1)
Fe(1)–C(5)	2.04(1)	Ru(1)–C(15)	2.22(1)
Fe(1)–C(6)	2.08(1)	Ru(1)–C(16)	2.22(1)
Fe(1)–C(7)	2.12(1)	Ru(1)–C(17)	2.10(1)
Fe(1)–C(8)	2.14(1)	Ru(1)–C(18)	2.15(1)
Fe(1)–C(9)	2.07(1)	Ru(1)–C(19)	2.15(1)
Fe(1)–C(10)	2.06(1)	Ru(1)–C(20)	2.16(1)
Fe(2)–C(23)	2.12(1)	Ru(2)–C(33)	2.19(1)
Fe(2)–C(24)	2.13(1)	Ru(2)–C(34)	2.19(1)
Fe(2)–C(25)	2.18(1)	Ru(2)–C(35)	2.10(1)
Fe(2)–C(26)	2.07(1)	Ru(2)–C(36)	2.21(1)
Fe(2)–C(27)	2.03(1)	Ru(2)–C(37)	2.10(1)
Fe(2)–C(28)	2.15(1)	Ru(2)–C(38)	2.25(1)
Fe(2)–C(29)	2.10(1)	Ru(2)–C(39)	2.25(1)
Fe(2)–C(30)	2.09(1)	Ru(2)–C(40)	2.17(1)
Fe(2)–C(31)	1.94(1)	Ru(2)–C(41)	2.18(1)
Fe(2)–C(32)	2.05(1)	Ru(2)–C(42)	2.23(1)
C(1)–C(21)	1.50(1)	C(6)–C(22)	1.53(2)
C(11)–C(21)	1.54(2)	C(16)–C(22)	1.56(1)
C(23)–C(43)	1.51(2)	C(33)–C(43)	1.45(2)
C(28)–C(44)	1.48(2)	C(38)–C(44)	1.41(2)

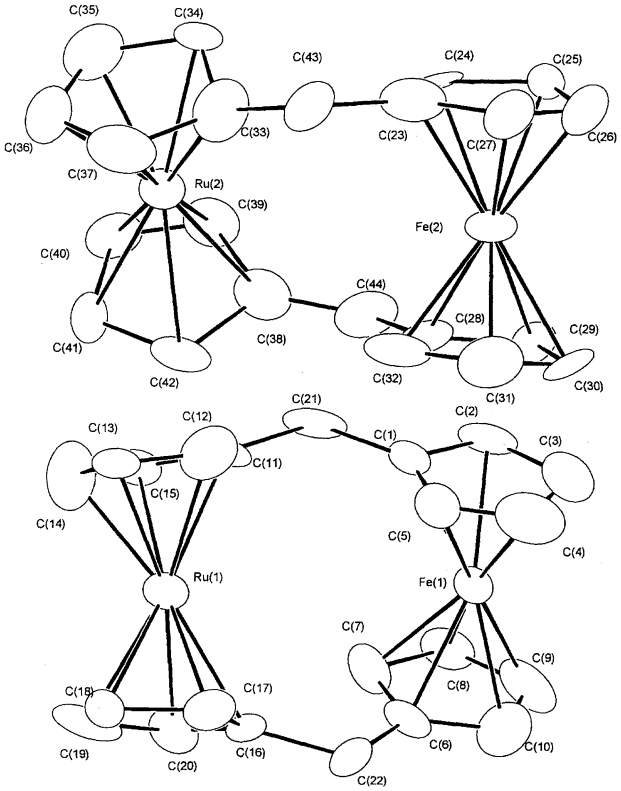

Fig. 5. ORTEP drawing of cations cation **A** (bottom) and cation **B** (top) for salt **4**.

metallocenophanium salt, although some neutral *anti*-[1.1]-metallocenophanes were reported.[11—13] In order to avoid a steric hindrance between the inner α-hydrogens, the *anti*-form of **4** adopts a more twisted structure than the *syn*-form of metallocenes **1**—**3**. The two $C_5H_4CH_2C_5H_4$ rings were strongly twisted. The twist angles (34.1°) for the planes C(1—5) and C(11—15) and that (38.2°) for the planes C(6—10) and C(16—20) were much larger than those of **2a** and **2b** and close to those in the *anti*-1,13-dimethyl[1.1]-ferrocenophane (36.1 and 34.0°[13]). Moreover, the largely tilted structure was found for the $Ru(C_5H_4)_2$ moieties of **4**, in which the tilt angle was found to be 12.7° (that for the $Fe(C_5H_4)_2$ moiety is 2.6°). Although the $Fe(C_5H_4)_2$ moiety is closely eclipsed (the rotation angles, about 5°), while the two Cp-rings of the $Ru(C_5H_4)_2$ moiety slide considerably from the eclipsed form (the rotation angles, about 14°). The large twisted and tilted structure of **4** gives the shorter Fe···Ru distance (4.608(2) Å for cation **A** and 4.597(2) Å for cation **B**) than the corresponding distances of **1a**, **2a**, **3a**, and **3b**. The distances between inner α-hydrogens were found to be 2.57 and 2.40 Å for H(5)–H(12) and H(7)–H(20), respectively, indicating no steric hindrance between them. The C_1–CH_2–C_1 angles were found to be 118(1)° and 121(1)° for C(1)–(21)–C(11) and C(6)–(22)–C(16), respectively.

The results obtained in these studies have established that the oxidation of the *syn*-[1.1]metallocenophane **2a** with H_2SO_4 under air gives the *anti*-formed salt **4**. This is in sharp contrast to the oxidation of **2a** with iodine reported previously,[23] in which the use of 1.5 molar amounts and a large excess and of iodine gave the monocationic $[Ru^{II}(C_5H_4CH_2C_5H_4)_2Fe^{III}]^+$ (**6**) and the dicationic $[I\text{–}Ru^{IV}(C_5H_4CH_2C_5H_4)_2Fe^{III}]^{2+}$ (**7**) with a direct Ru–I bond, respectively. From their X-ray diffraction studies, the conformation of both cations was *syn* form.

To investigate the above mentioned conformational change from *syn* to *anti* form found in **4**, the oxidation of **2b** with concd H_2SO_4 was done under the same conditions as for preparation **4**. The yellow color of the solution dissolved of **2b** in concd H_2SO_4 changed to blue-green immediately, and then gas was evolved. On addition of an aqueous solution of NH_4PF_6, the salt **8** was formed from the solution. The reaction is comparable to the reaction of **2b** with BF_3·HOH reported previously (e.g., formation of hydrogen gas), which gives the α-carbocation formulated as $[Fe(C_5H_4CH_2C_5H_4)(C_5H_4CH^+C_5H_4)Fe]BF_4^-$. The stability of the carbocation $\mathbf{2b}^+$ is ascribed to delocalization of the positive charge (each Fe atom takes up one-third of the positive charge and the other charge sits on the CH^+ group) based on the results of ^{57}Fe-Mössbauer study (a much smaller quadrupole splitting 1.80 mm s^{-1} value was found).[24] The Mössbauer study of **8** is comparable with those of the α-carbocation $\mathbf{2b}^+$ salt. For example, the quadrupole splitting and isomer shift values were found to be 1.58 and 0.40 mm s^{-1} at 300 K and 1.61 and 0.45 mm s^{-1} at 78 K, respectively, indicating the salt **8** is an α-carbocation salt. The NMR study of **8** supports the above the result. The eight signals of ring protons (δ = 6.05, 5.72, 5.25, 5.20, 4.65, 4.31, 4.29, 3.82), two signals of methylene (δ = 2.58 and 2.50) and the sharp CH^+ signal at lower field (δ = 7.75) were obtained for **8** in CD_3CN. Thus, the PF_6 salt **8** is not the [1.1]ferrocenophanium salt formulated as $[Fe^{II}(C_5H_4CH_2C_5H_4)_2Fe^{III}]^+PF_6^-$ but the α-carbonium salt $[Fe(C_5H_4CH_2C_5H_4)(C_5H_4CH^+C_5H_4)Fe]PF_6^-$, suggesting the CH_2 group of **2b** was easily oxidized in H_2SO_4 under air.

Considering of these facts, the driving force of conformational change from syn to *anti*-form by the oxidation in H_2SO_4 under air found in salt **4** may due to the bond formation of Ru and α-carbonium cation; i.e., the methylene group of **2a** is first oxidized by the oxidation giving the α-carbonium cation, formulated as $[Fe(C_5H_4CH_2C_5H_4)(C_5H_4CH^+C_5H_4)Ru]$ **5**. The cation is stabilized by the bond formation between the Ru atom and the carbonium center and the structure was already verified by X-ray diffraction.[9] The presence of the Ru–CH^+ bond may result in the conformational change from the *syn*-form to the *anti*-one. When water is added to the solution, the Fe^{II} in the $Fe(C_5H_4)_2$ moiety may be oxidized by the –CH^+– fragment with the cleavage of the Ru–CH^+ bond because of the lower oxidization potential of the Fe atom although the detailed mechanism of them have not been established, however the driving force of the conformation change must be due to the formation of the Ru–CH^+ bond. The absence of the softer Ru atom in **2b** would preserve the *syn*-form of the α-carbonium salt **8**; i.e., no conformational change was occurred. To prove this conclusion, further studies such as X-ray diffraction of the *anti*-form of **2a** which may be prepared by the reduction of **4** and the details of the mechanism of conformational change from *syn* to *anti* observed for **4** are required.

References

1) U. T. Mueller-Westerhoff, *Angew. Chem., Int. Ed. Engl.*, **25**, 702 (1986).

2) U. T. Mueller-Westerhoff, A. Nazzal, W. Prossderf, J. J. Mayerle, and P. L. Collins, *Angew. Chem.*, **94**, 313 (1982); *Angew. Chem., Int. Ed. Engl.*, **21**, 293 (1982).

3) U. T. Mueller-Westerhoff, A. Nazzal, and W. Prossderf, *J. Am. Chem. Soc.*, **103**, 7678 (1981); U. T. Mueller-Westerhoff and A. Nazzal, *J. Am. Chem. Soc.*, **106**, 5381 (1984).

4) U. T. Mueller-Westerhoff, T. J. Haas, G. F. Swigers, and T. K. Leipert, *J. Organomet. Chem.*, **472**, 229 (1994); U. T. Mueller-Westerhoff, A. Nazzal, and M. Tanner, *J. Organomet. Chem.*, **236**, C41 (1982).

5) T. H. Barr, H. L. Lentzner, and W. E. Watts, *Tetrahedron*, **25**, 6001 (1969).

6) J. Katz, N. Acton, and G. Marin, *J. Am. Chem. Soc.*, **95**, 2934 (1973); J. Katz, N. Acton, and G. Marin, *J. Am. Chem. Soc.*, **91**, 2804 (1969).

7) A. L. Rheingold, U. T. Mulleller-Westerhoff, G. F. Swiegers, and T. J. Haas, *Organometallics*, **11**, 3411 (1992).

8) M. Löwndahl, Ö. Daridsson, and P. Ahlerg, *Organometallics*, **12**, 2841 (1994).

9) M. Watanabe, I. Motoyama, and T. Takayama, *J. Organomet. Chem.*, **524**, 9 (1996); M. Watanabe, I. Motoyama, and T. Takayama, *Bull. Chem. Soc. Jpn.*, **69**, 2877 (1996).

10) W. E. Watts, *J. Am. Chem. Soc.*, **88**, 856 (1966).

11) A. Clearfield, C. J. Simmons, H. P. Witheres, Jr., and D. Seyforth, *Inorg. Chim. Acta*, **75**, C45 (1983).
12) J. Park, Y. Seo, S. Cho, D. Whang, K. Kim, and T. Chang, *J. Organomet. Chem.*, **489**, 23 (1995).
13) M. Löwndahl, Ö. Daridsson, P. Ahlberg, and M. Håkansson, *Organometallics*, **12**, 2417 (1993).
14) M. Watanabe and H. Sano, *Bull. Chem. Soc. Jpn.*, **63**, 777 (1990).
15) J. D. Dunitz, L. E. Oregel, and A. Rich, *Acta Crystallogr.*, **9**, 373 (1956); P. Seiler and J. D. Dunitz, *Acta Crystallogr., Sect. B*, **B28**, 1331 (1972).
16) G. L. Hardrove and D. H. Templeton, *Acta Crystallogr.*, **12**, 28 (1959).
17) J. S. Mckechnie, C. A. Marie, B. Bersted, and I. C. Paul, *J. Chem. Soc., Perkin Trans.*, **1973**, 2, 138.
18) L. Pauling, "The Nature of the Chemical Bond," 3rd ed, Cornell Univ. Press (1960).
19) N. D. Jones, R. E. Marsh, and J. H. Richards, *Acta Crystallogr.*, **19**, 330 (1965).
20) F. A. Cotton and G. Wilkinson, "Advanced Inorganic Chemistry," 5th ed, John Wiley and Sons, Inc., New York (1988), pp. 90—94.
21) M. Sato and M. Asai, *J. Organomet. Chem.*, **430**, 105 (1992).
22) N. J. Mammano, A. Zalkin, A. Landers, and A. L. Rheingold, *Inorg. Chem.*, **16**, 297 (1977).
23) M. Watanabe, I. Motoyama, and H. Sano, *J. Organomet. Chem.*, **510**, 243 (1996).
24) U. T. Mulleller-Westerhoff, A. Nazzal, W. Prossderf, J. J. Mayerle, and R. L. Collins, *Angew. Chem., Suppl.*, **1982**, 686.